# Active Polymers for Renewable functional Actuators (APRA)

Liquid crystalline elastomers (LCE) make a remarkable class of materials.[1] However, most of the research and application interest is focused on LCE actuators and artificial muscles[2,3]. The APRA project has its main focus on the further development of these actuators and their practical applications — but in the process of our work, we came across two very different, and previously unknown physical responses of LCE. This article introduces these two new effects: the enhanced dynamic adhesion on a surface of nematic LCE, and the reversible control of friction on a surface of an LCE composite with fabric.

## 1. Enhanced dynamic adhesion in nematic LCE

Smart adhesives that undergo reversible detachment in response to external stimuli enable a wide range of applications in household products, medical devices, or manufacturing. Here a new model system for the design of smart soft adhesives that dynamically respond to their environment is presented. By exploiting the effect of dynamic soft elasticity in nematic LCE, the temperature-dependent control of adhesion to a solid glass surface is demonstrated. The adhesion strength of LCE is more than double in the nematic phase, in comparison to the isotropic phase, further increasing at the higher detachment rates. The static work of adhesion, related to the interfacial energy of adhesive contact, is shown to change very little within the explored temperature range. Accordingly, the observed enhanced adhesion in the nematic phase is primarily attributable to the increased internal energy dissipation during the detachment process. We correlate this adhesion effect with the inherent bulk dynamic-mechanical response in the nematic LCE. The reported enhanced dynamic adhesion could lead to the development of a new class of stimuli-responsive adhesives.

In many applications of soft polymeric materials, the adhesive properties are important. In particular, pressure-sensitive adhesives[4] (PSA) form a class of applications of viscoelastic polymers, including elastomers and gels, which generally provide quick adhesion after applying light pressure, and detachment in some situations. However, in general, a polymer surface has fixed properties, being either sticky or non-sticky, and this varies only slightly and monotonically with environmental conditions such as humidity or temperature. Thus, such general polymers are not suitable for 'smart' applications that require both adhesion and its release upon demand. Thus, the design of the system with dynamic adhesive characteristics, e.g. with small temperature change, is an important target in materials design.

Many systems have been proposed to have a (desirably) sharp transition of adhesive characteristics in response to various stimuli, mainly affecting the interfacial energy density via the bare surface tension of each material or chemical/physical bond/entanglements.[5] However, less attention has been paid to the use of the bulk viscoelastic characteristics, which are especially important in dynamic applications, towards stimuli-responsive adhesives.[6] To our knowledge, no experimental study exists of the switchable adhesion of the nematic liquid crystal elastomers (LCEs), which do possess unique bulk mechanical properties. Apart from the celebrated spontaneous and reversible actuation, the other unique characteristics of nematic LCE, on which we especially focus here, is the effect of soft elasticity,[7] which in dynamic-mechanical setting manifests itself in a large increase in the loss factor $tan\delta$, and the decrease in the storage moduli $E'$ and $G'$.[8] This effect shows a great potential in LCE as energy damping materials.[9] Importantly, these viscoelastic properties are known to have a close relationship with the performance of adhesives. As these properties can vary sharply across the nematic-isotropic transition in LCE, we expect them to alter the adhesion characteristics as well.[10]

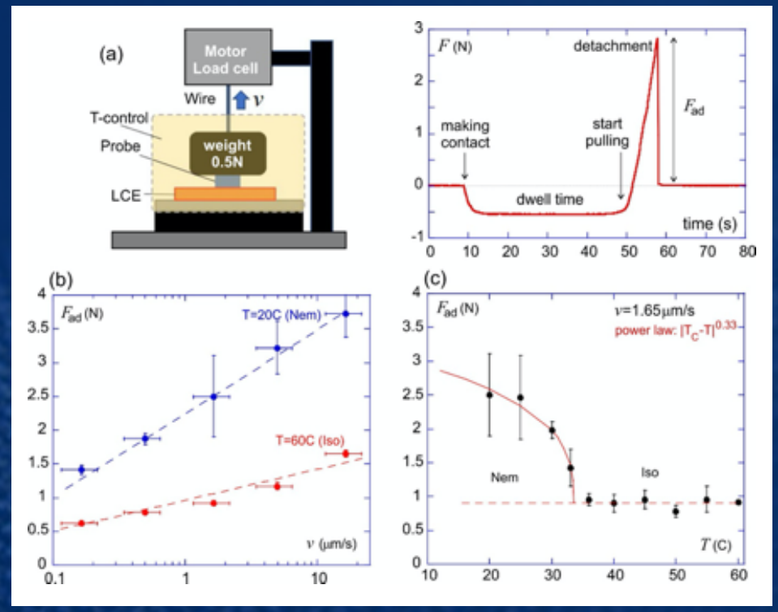


*Figure 1: Dynamic adhesion on LCE: (a) Schematic of the probe-tack apparatus. After a flat glass surface with the squared shape probe, is first pressed into the LCE surface at 0.5 N for ~30 s, the probe is pulled back with a pulling speed of motor, vm, and force is monitored. A typical force vs time curve at v=1.65 μm/s is shown on the right. Positive force indicates that required to detach the probe from the sample. Adhesive forces are read as the maximum of curves, labelled by $F_{ad}$. (b) Plots of $F_{ad}$ vs v, which is the probe speed estimated from the compliance of the apparatus, at RT and HT. (c) Plots of $F_{ad}$ vs T at v=1.65 μm/s. The curve fitted to a power law toward the critical temperature, (Tc-T)1/3, is also shown for guidance. The arrow indicates the microscopic director direction.*

The adhesion of the polydomain nematic LCE was tested via the probe-tack experiment (Figure 1a). Our material was designed to have relatively low TNI, which makes adhesion experiments more practical within the temperature range of 20~60°C, and better suitable for applications, including household and biomedical products. Figure 1b shows a typical force curve obtained by the probe-tack test using the thin LCE film, with the thickness of d=0.1 mm, and the probe area of 25 $mm^2$. In our experiments, the sharp drops of the monitored force were always observed, and the repeated probe-tack curves were highly reproducible, indicating the interfacial detachment without fatal fracture of the bulk LCE under the present test conditions.

The maximum force required to detach the probe from the sample is defined as the 'adhesion strength', and its dependency on the probe speed relative to the sample is shown in Figure 1b, comparing the room temperature (RT, 20°C) and a high temperature (HT, 60°C). The force ratio is about 3 here, although our best materials reached the ratio of 7. The temperature dependence of $F_{ad}$, shown in Figure 1c, indicates that the adhesion strength is closely related to the phase behaviour of the LCE. The LCE is nematic at RT, and isotropic at HT, which is confirmed by the dynamic scanning calorimetry (Figure 2a) and wide-angle X-ray scattering. The probe-tack test results show a tangible difference in the adhesion between the two different phases. Although the physical relationship between the nematic order parameter and the adhesion is not yet established, it is noteworthy that the curve roughly follows the critical behaviour of the phase transition of the nematic LCE. The temperature-dependent adhesion has also been demonstrated on a different peeling experiment, called a 90°-peel test with constant force. The adhesion is strong in the nematic phase; the peeling starts near $T_{NI}$, and accelerates on further elevating temperature in the isotropic phase, showing a good example of stimuli-responsive detachment on a smart soft

1 Warner and Terentjev (2007) Liquid Crystal Elastomers, Oxford University Press.
2 Küpfer, Nishikawa and Finkelmann (1994) Polym. Adv. Technol. 5 110
3 Tajbakhsh and Terentjev (2001) Euro. Phys. J. E 6 181
4 Creton and Ciccotti (2016) Rep. Prog. Phys. **79**, 46601.
5 De Crevoisier, Fabre, Corpart and Leibler (1999) Science, **285**, 1246
6 Ito, Akiyama, Sekizawa, Mori, Yoshida and H. Kihara (2018) ACS Appl. Mater. Interfaces, **10**, 32649.
7 Warner, Bladon and Terentjev (1994) J. Phys. II France, **4**, 93.
8 Clarke, Tajbakhsh, Terentjev and Warner (2001) Phys. Rev. Lett. **86**, 4044.
9 Clarke, Tajbakhsh, Terentjev, Remillat, Tomlinson and House (2001) J. Appl. Phys. **89**, 6530.
10 Corbett and Adams (2013) Soft Matter, **9**, 1151

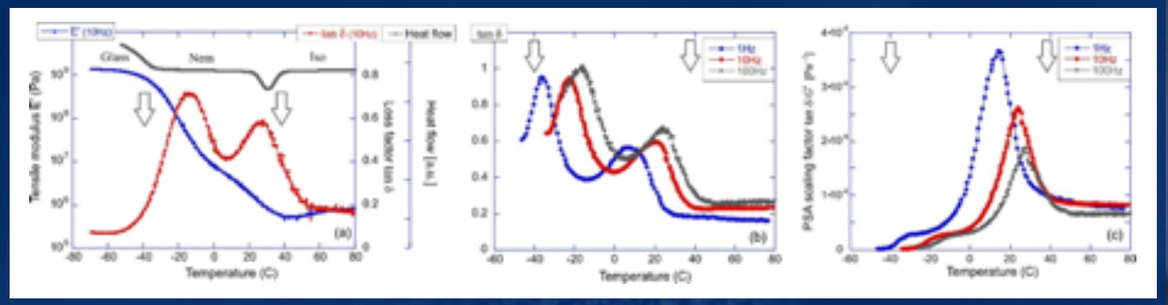


*Figure 2: Dynamic soft elasticity in LCE: (a) The tensile storage modulus E′, and the loss factor tanδ, at a fixed frequency of 10 Hz, on sample cooling at 3°C/min. The graph also shows the DSC scan, illustrating the nematic and the glass transition temperatures (marked by arrows in all three plots). (b) The frequency dependence of the dynamic transitions, illustrated by the loss factor, on sample cooling. (c) The frequency-dependent scaling factor tanδ/G′ for PSA, illustrating the major role of the internal dissipation in the nematic phase.*

adhesive. We have confirmed that this temperature-dependent adhesion is fully repeatable, at least after ten heating-cooling cycles.

The dynamic-mechanical test results shown in Figure 2 indicate the characteristic large increase of the loss factor in the nematic phase (the effect of dynamic soft elasticity). By increasing the test frequency, which roughly corresponds to the increase of peeling velocity *v*, the loss factor within the nematic range also increases (Figure 2b). This directly correlates with the increase of adhesion (Figure 1b). Although there still a need for detailed experiments and a proper theory for the full understanding of this problem, we may conclude that the observed strong temperature dependence of adhesion is attributed to the drastic changes in the viscoelastic loss in the LCE.

The DMA tests also show large values of *tanδ* at low temperatures, which corresponds to the glass transition region (Figure 2). Although it is tempting to follow the previous logic, and suggest that the glass transition region is also useful to increase adhesion, in practice, this is not the case. There is a lot of literature in the general field of pressure-sensitive adhesives, where the scaling gauge is developed to estimate the performance of materials. It is established that the ratio $tan\delta/G'$ is most useful for this purpose[11] (see Figure 2c). Therefore, the large modulus in the glassy region suppresses the effective adhesion strength, in spite of the rise in the loss factor around $T_g$. In contrast, the storage modulus changes little between the nematic and isotropic phases of the elastomer. If anything, there is a decrease of $G'$ and $E'$ in the nematic phase close to the $T_{NI}$ (as shown in Figure 2a), which further enhances the effect on adhesion. This discussion suggests that the LCE in the nematic phase is a good candidate as a pressure-sensitive adhesive and, additionally, the high adhesion can be switched-off on changing the phase.

In conclusion, we found that the adhesion of solids to a surface of nematic LCE can be changed drastically by small changes in temperature, when it crosses between the nematic and isotropic phases, exploiting the inherent bulk viscoelastic properties of the nematic LCEs. It is possible to modulate $T_{NI}$, $G'$ and $G''$, and the surface chemistry through the variation of material components. For instance, $T_{NI}$ can be increased by decreasing the amount of non-mesogenic spacers, and $G'$ can be lowered by decreasing the amount of the crosslinker. The nematic-isotropic phase transition can also be induced by other stimuli, for example, light and chemicals,[1] by incorporating the molecular units sensitive to them in the polymer formulation. This makes the reported mechanism of reversible viscoelastic damping applicable in a broad class of smart switchable soft adhesives toward, household, biomedical, and manufacturing applications.

## 2. Dynamic manipulation of friction in smart LCE-textile composites

Smart surfaces that reversibly change the interfacial friction coefficients in response to external stimuli enable a wide range of applications, such as grips, seals, brake pads, packaging films, and fabrics. Here we describe a new concept of such a smart frictional system: a composite film of a plain-weave polyester textile sheet, and a thermo-responsive nematic liquid crystalline elastomer (LCE). The composite is deployed with retractable micro-undulations of the elastomer inside each weave mesh, enabling dramatic changes of the contact interface with the opposing surface on LCE actuation, which is induced, e.g. by a change in temperature. At room *T*, the protruding viscoelastic parts of LCE in the nematic phase make contact with the opposing flat surface, resulting in very high friction. At an elevated *T* (in isotropic phase), the undulations of LCE surface are retracted within the thickness of the textile, and the contacts are limited to small regions around overlapping textile fibres, lowering the friction dramatically. This effect is fully reversible on heating/cooling cycles.

Our system is the composite (Figure 3) of a nematic LCE and a plain-weave textile, in which the volume other than the fibre components within the thickness of the textile is almost fully filled with the LCE, as in the rubber-coated textiles. The basic properties of the present LCE were: $T_{NI}$=35°C, spontaneous and reversible changes of the shape with the uniaxial strain of at least 30%, and of the soft viscoelasticity with the high loss factor *tanδ* in the nematic phase. The fabrication of the composite begins with moulding the LCE precursor and the textile sheet between two flat glass slides under normal pressure, and its thermal curing in the isotropic phase (Figure 3a). The first thiol-ene reaction, creates a random isotropic polymer network. During annealing of the peeled free-standing sample, the solvent is evaporated, causing the volumetric shrinkage. Since the textile lattice is locally rigid, the shrinkage occurs exclusively in the direction normal to the sample plane (Figure 3b), which is different from the neat LCE systems without constraints of the textile frame. Then, the sample is uniaxially stretched at RT (in the nematic state) to the strain of 30% in the diagonal direction of the square mesh openings, which is the most compliant direction (x) of the plain-weave textile. Under this strain, the LCE parts at mesh openings adopt a buckled surface structure in response to the induced local compressive strain of approximately -45% in the orthogonal direction (y) (Figure 3c).

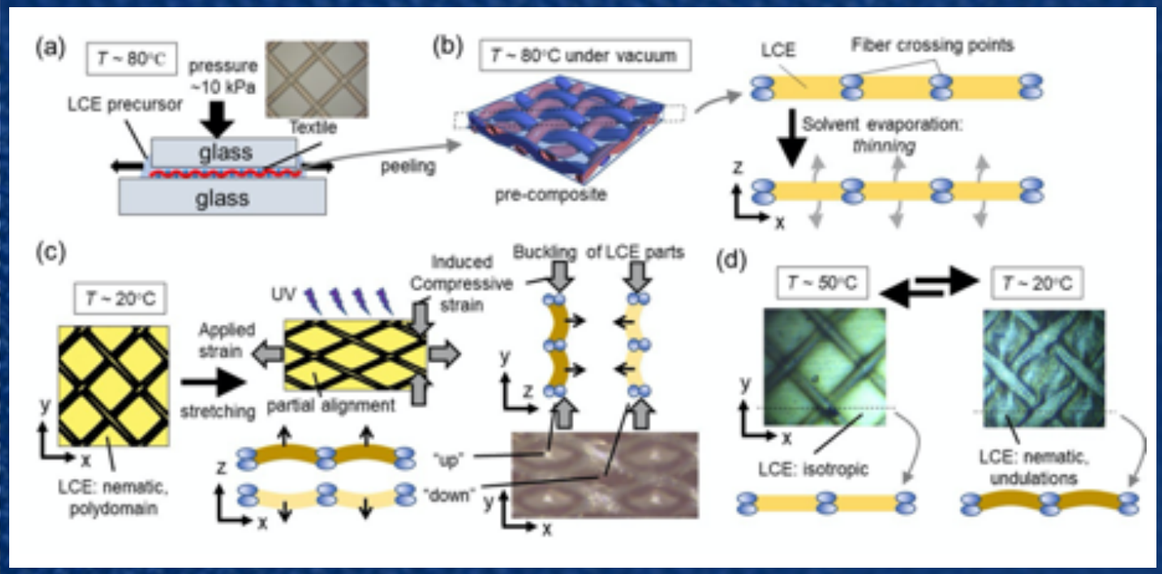


*Figure 3: Preparation of the LCE-textile composite sheet with micro-shape-changeability: (a) The LCE precursor with the textile between two glass slides undergoes the first cross-linking reaction at elevated temperature (isotropic phase). (b) Drying the peeled sample under vacuum, prompting solvent evaporation and volume contraction. (c) The second network crosslinking by UV irradiation under local uniaxial strain at RT (nematic phase). The LCE parts buckle protruding in one of the out-of-plane directions, 'up' or 'down', alternatively along the nearest neighbouring mesh openings. This structure is 'memorised' by the secondary crosslinking in the nematic phase. (d) Release of applied tensile strain and annealing in isotropic phase causes restoring of the original shape, memorised in the isotropic state of LCE and the original textile shape with the square mesh opening. After cooling back to RT, the further modulated undulations of LCE segments appear due to the mismatch between the square shape of the mesh and the secondary memorised shape.*

After the second photo-crosslinking, the applied strain is released and the sample is annealed to equilibrate in a load-free state (Figure 3d). At HT, the original memorised state of the isotropic LCE is restored, and the original textile shape with square mesh opening is also recovered. After cooling back to RT, the modulated undulations of LCE segments, reflecting those formed under the applied strain, appear without changing the square shapes of the mesh. Owing to the mismatch between the naturally square shape of the mesh openings, and the rhombic shape recorded in the nematic phase, additional buckling of the elastomer surface occurs in response to the emerging compressive strain in the *x*-direction. Since the initial undulations can assist in nucleating the additional buckling, the initial buckling directions memorised under applied strain are retained in the structure. Upon heating again to $T>T_{NI}$, the undulations retract, restoring the state of the first crosslinked network. Consequently, the temperature change induces reversible alternation of micro-undulations only, while the macroscopic shape of the composite sheet remains constant.

Since buckling of the LCE segments is the key phenomenon behind the micro-undulations, the effective aspect ratio, (lateral length)/(thickness), of the LCE segments in the mesh openings is an important parameter, which depends on the mesh size. In our main study, the composites of the textile with the mesh opening of 0.199 mm (T100) were used as the representative system with ideal micro-undulations. The detailed temperature-dependent surface topographies are shown in Figure 4. The undulations of the LCE parts in the mesh openings at RT (nematic) are retracted at HT (isotropic) toward the mid-plane of the sample sheet.

11 Wang, Colver, Bon and Keddie (2009) Soft Matter, 5, 3842.

The amount of the solvent during the preparation, $c_{sol}$, affects the surface topography via the final thickness of the LCE layer. In particular, it controls the height difference h between the fibre-crossing points and the LCE parts (Figure 4g,h). At HT, h linearly increases at ~0.5 μm/wt% as shown by the red dashed line in Figure 4h. Since the textile half-thickness is 50 μm, the result indicates that the shrinkage of LCEs near the centre of the mesh opening occurs mainly in the direction perpendicular to the film. The non-zero value of $h$ at $c_{sol}$ = 0 wt% would be due to the non-negligible curing shrinkage (syneresis). At RT, values of $h$ become smaller due to the micro-undulations at LCEs. The transformation between two states is fully repeatable over many cycles, as expected from the neat sample and the other nematic LCEs.

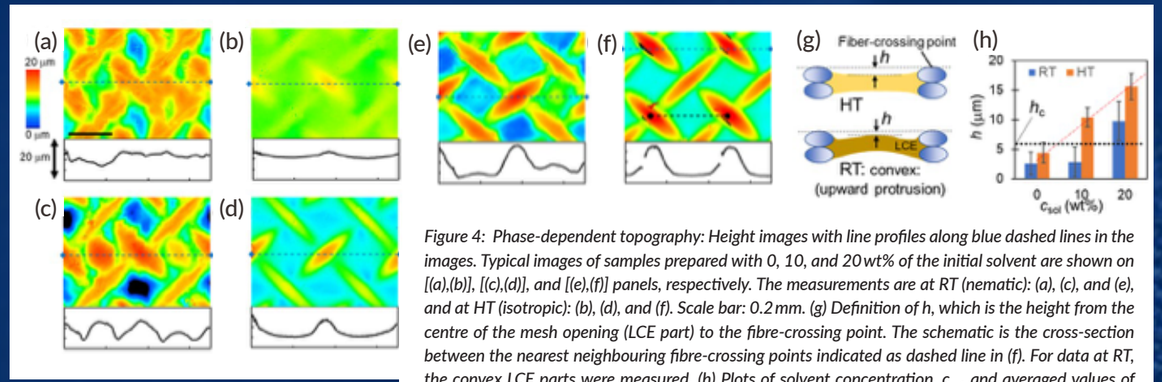


*Figure 4: Phase-dependent topography: Height images with line profiles along blue dashed lines in the images. Typical images of samples prepared with 0, 10, and 20 wt% of the initial solvent are shown on [(a),(b)], [(c),(d)], and [(e),(f)] panels, respectively. The measurements are at RT (nematic): (a), (c), and (e), and at HT (isotropic): (b), (d), and (f). Scale bar: 0.2 mm. (g) Definition of h, which is the height from the centre of the mesh opening (LCE part) to the fibre-crossing point. The schematic is the cross-section between the nearest neighbouring fibre-crossing points indicated as dashed line in (f). For data at RT, the convex LCE parts were measured. (h) Plots of solvent concentration, $c_{sol}$, and averaged values of h obtained from images with the larger area at multiple locations (N > 10). The characteristic height value, $h_c$=6 mm, dividing the two contact regimes described later, is shown as a guidance.*

The static, $F_S$, and kinetic friction forces, $F_K$, between the LCE-textile composite and the flat glass surface were investigated (Figure 5a) at relatively weak load $L$ < 1 N, for which the deformation of the PE fibre at the overlapping point is negligible. The typical time-dependent frictional signals are shown in Figure 5b, in which $F_S$ and $F_K$ are defined. The temperature-dependent static and kinetic friction coefficients, $\mu_S$ and $\mu_K$, (Figure 5c,d) are obtained as slopes of the linearly fitted line to the $L$-dependent friction (Figure 3e,f). They are roughly classified as either the higher ($\mu_S$ > 1, $\mu_K$ > 0.6) or lower ranges ($\mu_S$ < 0.4, $\mu_K$ < 0.2). According to the observation of contact regions, the high friction corresponds to the states with the larger contact area consisting of LCE parts. In the low friction case, contacts only occur at points of overlapping fibres, with small area. In particular, the sample prepared with 10 wt%-solvent shows maximum $T$-dependent changes in both $\mu_S$ and $\mu_K$, each of which shows almost six-fold increase on cooling from HT to RT. For comparison, the best results on the increase of friction in a LC polymer layer were at most 2-fold, and only when two patterned surfaces were against each other. In the deformation-induced wrinkled bilayer surface the friction increase was at most 1.5-fold, see the review[12] for detail. The results demonstrate the effectiveness of the present composite design with $T$-dependent topographical changes on the dynamic friction.

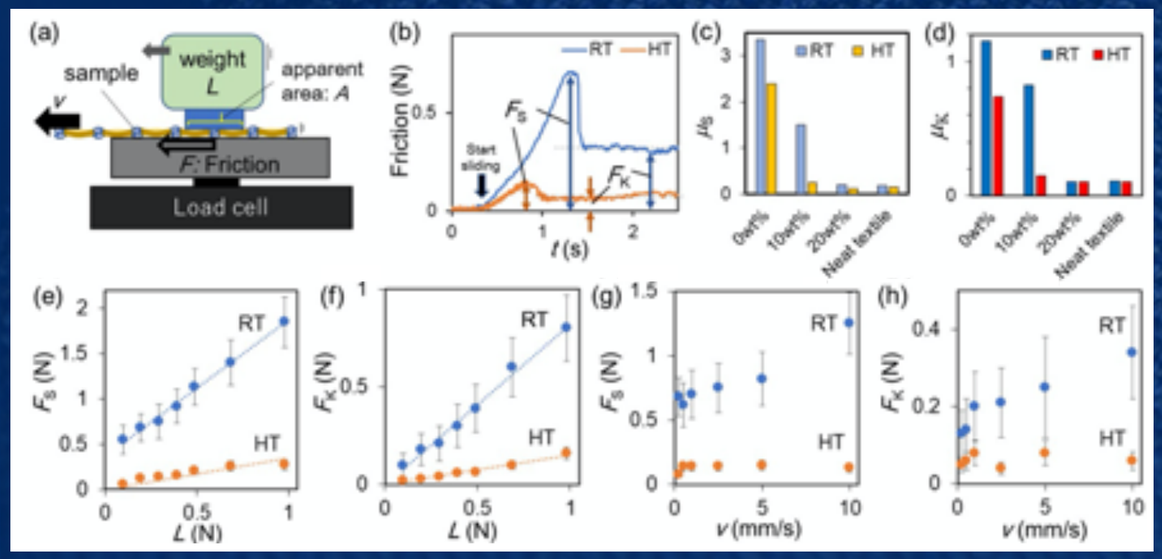


*Figure 5: Friction tests: (a) Schematic for friction tests. (b) Example of the friction signal and the definition of static and kinetic frictions, $F_S$ and $F_K$, respectively. The data on the sample prepared with 10 wt% solvent at v= 5 mm/s with load L = 0.3 N (apparent normal pressure of 2.2 kPa) are shown. (c) Static, $\mu_S$, and (d) kinetic, $\mu_K$, friction coefficients, obtained as slopes of plots of friction force vs normal load. (e)-(h) Plots of friction on composite prepared with solvent at 10 wt%. Plots of (e) $F_S$, and (f) $F_K$, vs normal load, L, at RT and HT. Plots of (g) $F_S$ and (h) $F_K$ vs sliding speed v, at RT and HT.*

In summary, here we report the design of LCE-textile composites with thermally retractable micro-undulations for the dynamic manipulation of friction coefficients via modulation of the contact states. The buckling-based spontaneous undulations of LCE parts in the openings of the textile mesh develop through a simple lithography-free procedure. The $T$-dependent interfacial contact states of the LCE-textile composites to a flat glass surface can be tuned by controlling the fine structure. With the optimised design, the LCE-textile composite makes contact at undulated viscoelastic LCE parts in the nematic phase at RT. In contrast, at HT, textile fibres at their crossing points mainly constitute the contacts with the small area. This alternation, which includes the changes in the contact area and replacement of the materials in contact, can modulate friction forces by sixfold. Owing to the simple fabrication of the transformable micro-structure, and the possibility of the further optimisation, including the fine structural modifications and tuning of LCE properties, the present design could provide a route to smart LCE-textile composite sheets and films that can reversibly change friction on demand. Since the textile provides the LCE with a better mechanical strength, while retaining the flexibility of a free-standing film, the present composite would also be promising for handling and further processing in a wide range of applications, e.g. robot hands, touch screen devises, and smart textiles.

12 Hu and Burgueño (2015) Smart Mater. Struct. **24**, 063001.

## SUMMARY

This project will bridge from the concept to technology, tuning the material design for robust nematic LCE vitrimers, impacting photo-actuation capacity with a controlled wavelength, and finally utilising them in practical-engineering actuator applications where the reversible mechanical action is stimulated by light, solvent exposure, or more traditionally – heat.

## PROJECT LEAD PROFILES

**Eugene Terentjev** studied in Moscow, obtaining the MSc in 1982 and PhD in 1985; then carried out postdoctoral research in Case Western Reserve University (Cleveland, Ohio). After moving to Cambridge in 1992, he became a University Lecturer in 1998 and Professor Terentjev authored over 300 original papers and reviews in a broad range of subjects in soft matter and biological physics.

## PROJECT PARTNERS

The APRA Project is coordinated from the University of Cambridge.

## CONTACT DETAILS

**Eugene M Terentjev**
+44 (0)1223 337003
emt1000@cam.ac.uk
www.europeandissemination.eu/apra-project-eugene-m-terentjev/2836

## FUNDING

APRA received funding from the European Union's Horizon 2020 Research and Innovation Programme ERC-2017-ADG under grant agreement no. 786659.